Int. J. Electrochem. Sci., 13 **(2018)** 3691 – 3699, doi: 10.20964/2018.04.46

International Journal of
ELECTROCHEMICAL
SCIENCE
www.electrochemsci.org

Effect of molar ratio of Li_2CO_3/MnO_2 on characteristic of the Lithium Manganate Synthesized via High Temperature Ball Milling Method

Qing Zhao[1,2], *Xuetian Li*[2,*], *Zhongbao Shao*[2], *Binshi Xu*[2], *Chengjun Liu*[1,2], *Maofa Jiang*[1,2]

[1] Key Laboratory for Ecological Metallurgy of Multimetallic Minerals (Ministry of Education), Northeastern University, Shenyang 110819, China
[2] School of Metallurgy, Northeastern University, Shenyang 110819, China
[*]E-mail: xuetian.li@163.com

Received: 16 December 2017 / *Accepted:* 5 February 2018 / *Published:* 6 March 2018

Lithium manganite ($LiMn_2O_4$) cathode materials were synthesized with Li_2CO_3, MnO_2 and polyethylene glycol 12000 as raw materials via high temperature ball milling method, and the effect of the value of the molar ratio of Li/Mn on the impurity, structure, morphology, and electrochemical performance was experimentally investigated in this work. Some impurity of $Li_{1.4}Mn_2O_4$ was detected in the L-1.15 (n_{Li}:n_{Mn} = 1.15:2), and the lithium source influenced the uniformity of particles. Some button batteries were assembled with the lithium manganite and the electrochemical performance was tested. L-1.1 (n_{Li}:n_{Mn} = 1.1:2) exhibited the optimal electrochemical performance: initial discharge capacities were 121.5, 109.5, 98.3, 86.5 and 70.2 $mAhg^{-1}$ at rates of 0.1, 0.5, 1.0, 2.0 and 5.0 C, respectively. After 100 cycles, the capacity was 89.5 $mAhg^{-1}$ at rate of 1.0 C and the capacity retention was 91.0%.

Keywords: Li-ion batteries; High temperature ball milling method; Lithium source; Electrochemical performance

1. INTRODUCTION

Li-ion batteries have attracted more attention because of the attractive characteristics such as high operating voltage, high particle density, long cycle life, low self-discharge, and no memory effect [1,2]. Cathode materials play a critical role in the performance of lithium ion battery. The lithium manganate ($LiMn_2O_4$) has become one of the most promising candidate cathode materials for Li-ion battery due to its low cost, abundant of available Mn resources, environmental friendliness and good safety as well as easy preparation [3-5]. However, the industrial application of $LiMn_2O_4$ is limited by

the cycling stability and rate performance [6]. To improve these electrochemical properties, some researches focus on the doping techniques [7,8] and surface modifications [9-11] has been recently devoted.

The tradition preparation methods used for synthesizing $LiMn_2O_4$ cathode material are solid-state reaction method [12-13], precipitation technique [14], hydrothermal method [15,16], microwave method [17], and sol-gel method [18]. Besides these methods, facile self-template method [19], spray-dried method [20], and micro-emulsion method [21] are also used to synthesize the $LiMn_2O_4$ with smaller particles, while these methods are usually regarded to be higher in cost and not environmentally friendly. Electrical storage capacity is determined by the amount of lithium ions inserted into electrodes for charge neutrality. However, evaporation loss of lithium usually occurs during the manufacturing process since the high synthesizing temperature [22]. Many electrode materials have been synthesized at a relatively low temperature by high temperature ball milling method by our research group [23-26]. In this work, $LiMn_2O_4$ were synthesized by the high temperature ball milling method, the influence of the value of the molar ratio of Li/Mn on the structure, morphology and electrochemical properties of $LiMn_2O_4$ was investigated.

2. EXPERIMENTAL

Lithium carbonate (Li_2CO_3, AR, 99.9%), electrolytic manganese dioxide (EMD) (MnO_2, 91%), and polyethylene glycol 12000 ($HO(CH_2CH_2O)_nH$, AR, 99.9%) were used as raw materials. Stoichiometric amounts of polyethylene glycol 12000 (5wt.% of the product mass) was dissolved in deionized water, and mixed with Li_2CO_3 and MnO_2 in different molar ratio of $n_{Li}:n_{Mn}$ = 1:2, 1.05:2, 1.1:2, and 1.15:2 (prepared samples are nominated as L-1, L-1.05, L-1.1, L-1.15, respecitvely). The slurry were then stirred by the stirrer for 2 h, and the precursor of lithium manganate was obtained after drying at 150 ℃ for 10 h in drying oven. The precursor was poured in a jar of high temperature ball milling equipment at a ball-to-powder mass ratio of 10:1. The synthesis process was performed at 600 ℃ for 8 h in the air atmosphere, after which lithium manganate powders were prepared. A flow sheet of the process route is given in Fig.1. The structure of the lithium manganate powders was characterized by X-ray diffraction (XRD, Rigaku D/max-RB) and the morphology was determined by scanning electron microscopy and energy-dispersive X-ray spectroscopy (SEM-EDS, HITACHI S-3000H) analysis.

The prepared lithium manganate materials, acetylene black and polyvinylidene fluoride (PVDF) binder were weighted according to the mass ratio of 80:10:10 and mixed, followed by adding some N-methyl pyrrolidone (NMP). The electrode slurry was coated on an Al foil and was then heated at 120℃ under vacuum for 12 h, the coated Al foil was cut into electrode disks (CR16 mm), which was used as an anode in the button battery assembling process that was conducted in an argon filled glove box. A lithium plate (CR15.8 mm) was used as the anode, and Celgard 2400 porous polypropylene screen was used as a membrane. Moreover, 1 M $LiPF_6$/EC+DEC (1:1 in volume) were employed as a liquid electrolyte in the battery.

Battery-testing system (Neware Co., Ltd., China) was adopted to test the cycle charge-discharge behavior for button battery product at different rates from 3.0 to 4.3V (1.0 C equals to 150 $mAhg^{-1}$). The cyclic voltammetry (CV) test was performed using CHI660E electrochemical work-station from 3.3 to 4.5V at a scan rate of 1.0 $mV \cdot s^{-1}$ at room temperature.

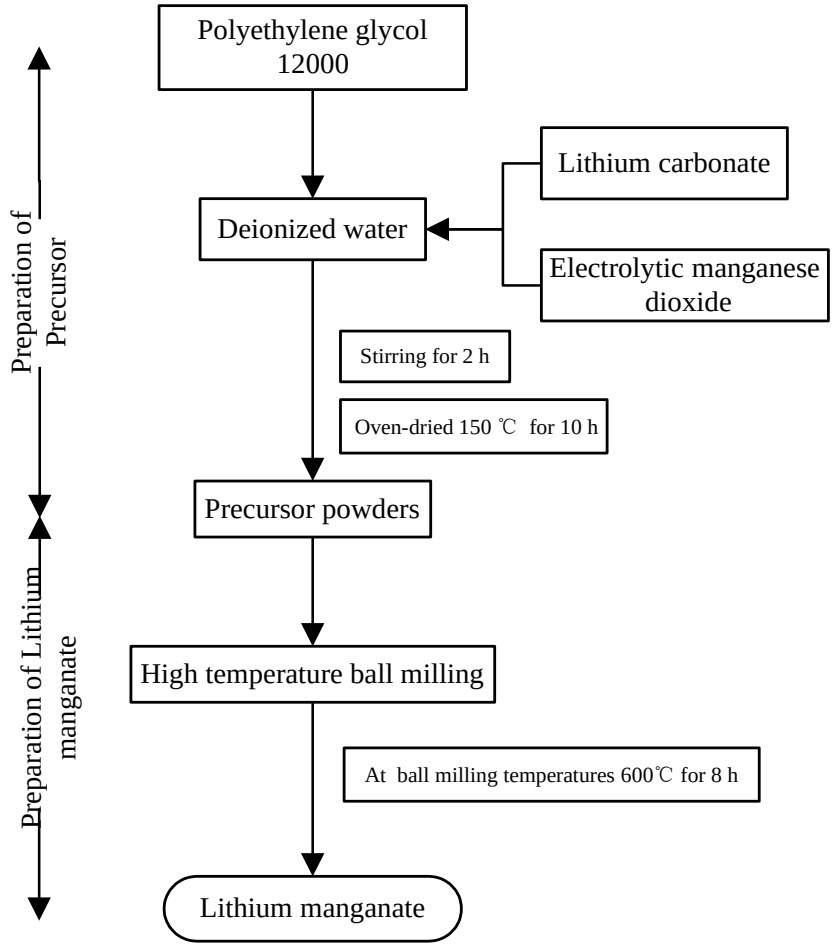

Figure 1. Flow sheet of the process route

3. RESULTS AND DISCUSSION

The XRD patterns of lithium manganate are provided in Fig. 2. It can be seen that obvious diffraction peaks of $LiMn_2O_4$ (spinel structure) were found in the four patterns, which were well indexed to *Fd3m* space group (JCPDS Card NO. 35-0782). It was demonstrated that the value of the molar ratio of Li/Mn more than 1:2 did not significantly affect the crystal structure of $LiMn_2O_4$. However, when the value of the molar ratio of Li/Mn was 1.15:2, some impurity of $Li_{1.4}Mn_2O_4$ was identified, which was also proved by EDS results. The surface morphology of lithium manganate samples were observed by SEM, which can be seen in Fig.3. Majority of the grain sizes of all the samples were around or smaller than 0.5 μm.

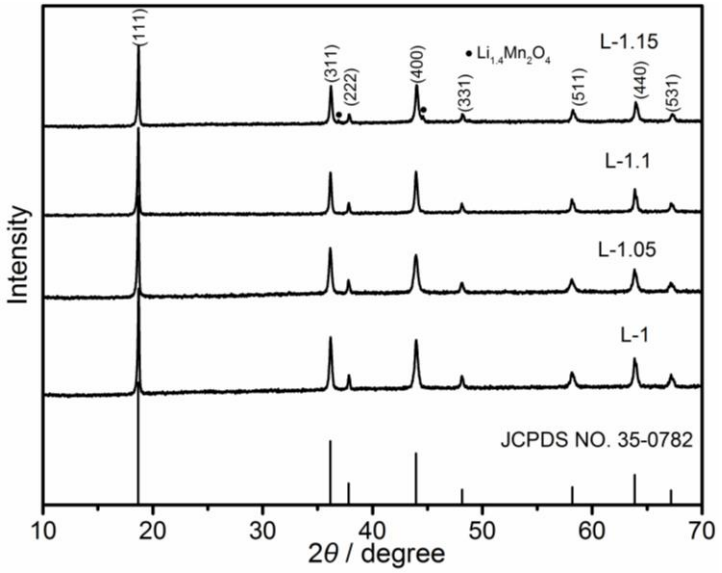

Figure 2. XRD patterns of lithium manganate prepared from different values of the molar ratio of Li/Mn (n_{Li}:n_{Mn} = 1:2, 1.05:2, 1.1:2, and 1.15:2, respectively).

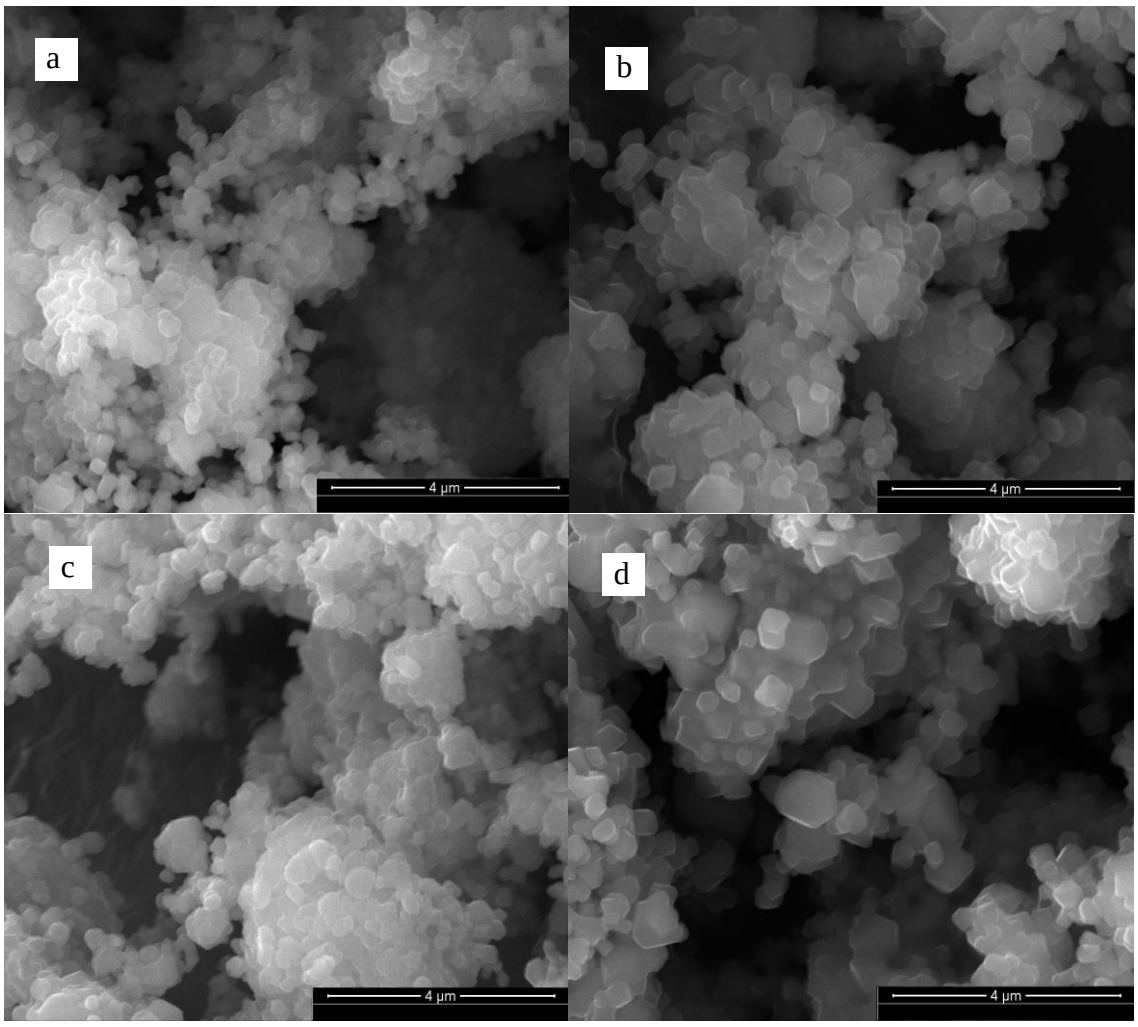

Figure 3. SEM images of lithium manganate prepared from different values of the molar ratio of Li/Mn (n_{Li}:n_{Mn} = (a) 1:2, (b) 1.05:2, (c) 1.1:2, and (d) 1.15:2, respectively).

Smaller particle size could provide a large surface area with a shorter path for Li^+ ion diffusion and large specific active area for electrochemical reaction [27]. Moreover, the particles exhibited a relatively uniform and regular shape when the value of the molar ratio of Li/Mn was 1.1:2.

Figure 4 (a) and (b) show the galvanostatic charge/discharge curves and cycling performance at 0.1C-rate of lithium manganate samples. The initial discharge capacities for the samples were 113.4, 115.5, 121.5 and 117.8 $mAhg^{-1}$ at a rate of 0.1C, respectively. After 50 cycles, the capacities of the samples remain at 95.9, 101.9, 113.3 and 102.9 $mAhg^{-1}$, and their capacities retentions were 84.6% , 88.2%, 93.3% and 87.4%, respectively. It was concluded that the Li-1.1 presented the largest discharge capacity and the best cycling performances among all of the samples. These results are attributed to the high purity and uniform morphology and grain size (cf. Figs. 2 and 3). Fig. 4 (c) shows the discharge capacities at various C-rates ranging from 0.1C to 5.0C of Li-1.1. The initial discharge capacities remain at 121.5, 109.5, 98.3, 86.5 and 70.2 $mAhg^{-1}$ at rates of 0.1, 0.5, 1.0, 2.0 and 5.0 C, respectively. Li-1.1 exhibited an excellent rate performance. Fig. 4 (d) shows the cycling performances of Li-1.1 sample at the rate of 1.0 C. After 100 cycles, the capacity of the sample remain at 89.5 $mAhg^{-1}$ at the rate of 1.0 C, and the capacity retention was 91.0%. Capacity decay is not obvious observed.

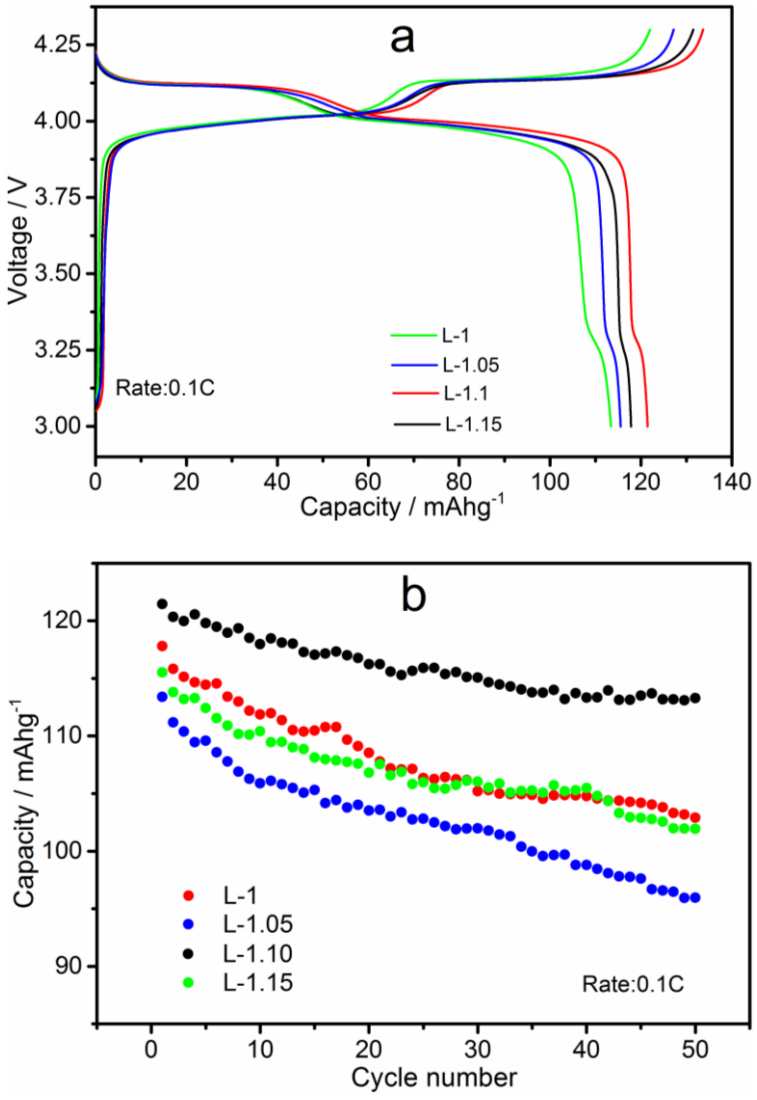

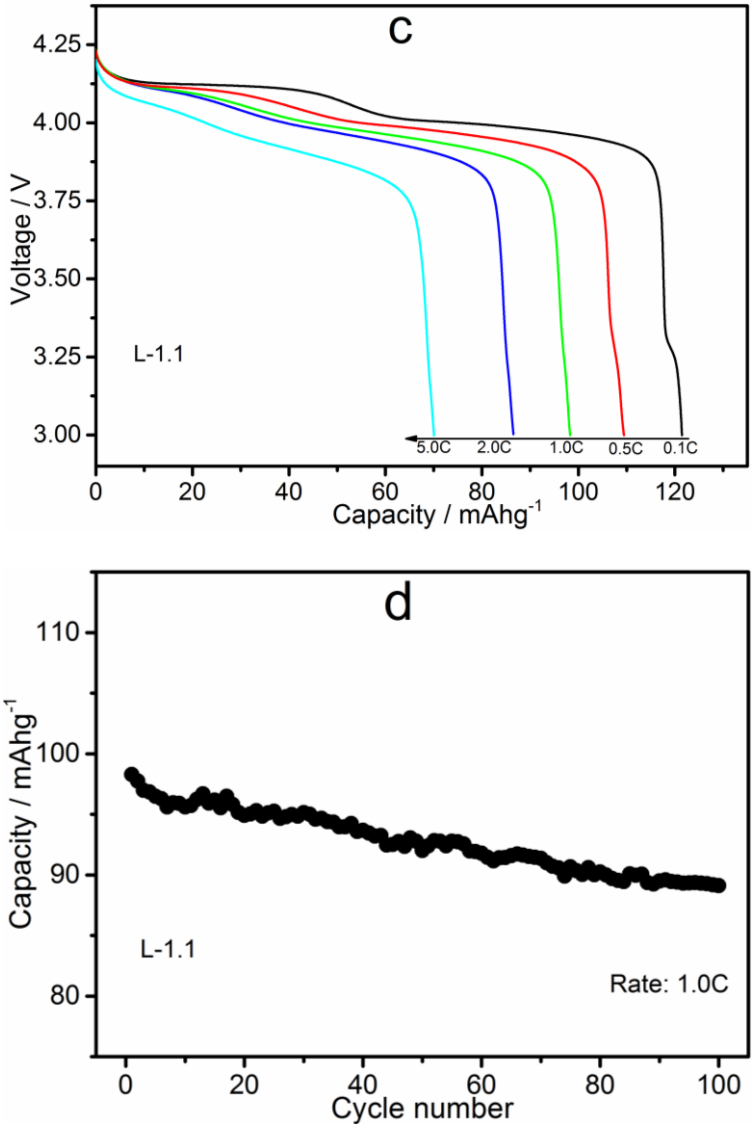

Figure 4. (a) Initial charge/discharge curves and (b) cycling performance at 0.1C-rate from 3.0 to 4.3V (Li^+/Li) of lithium manganate prepared from different values of the molar ratio of Li/Mn (n_{Li}:n_{Mn} = 1:2, 1.05:2, 1.1:2, and 1.15:2, respectively); (c) discharge capacities at various C-rates ranging from 0.1C to 5.0 C and (d) cycling performance at 1.0 C-rate of Li-1.1.

To investigate this further, the cyclic voltammetry measurement was conducted to analyze the oxidation and reduction processes during the charge-discharge cycles. Fig. 5 shows the testing results of lithium manganate samples from 3.3 to 4.5 V at a scan rate of 1.0 mVs^{-1}. It was indicated that all of the samples had two pairs of oxidation peaks and reduction peaks with a good symmetry, demonstrating that the electrochemical intercalation and de-intercalation reactions of lithium-ion proceed in two steps and the battery in the charge and discharge process reversible [28, 29]. These findings are strongly consistent with two plateau potentials of the charge-discharge capacity curves in Fig. 4 (a). Peak parameters of cyclic voltammetry curves for samples were summarized in Table 1.

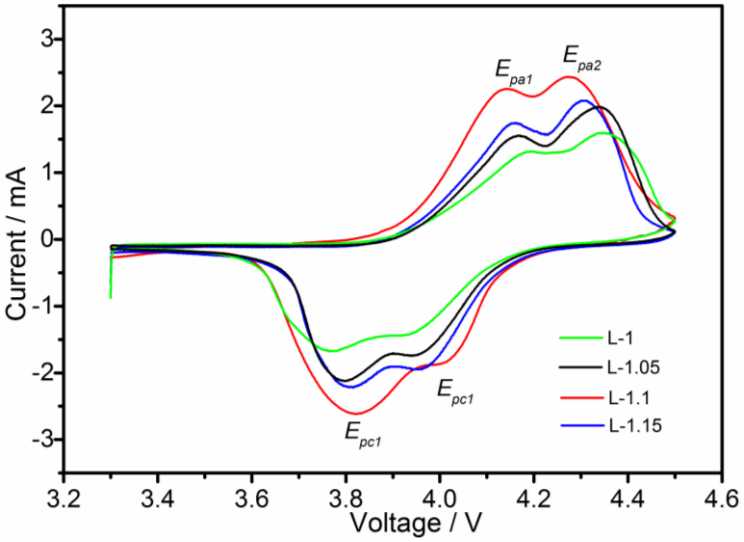

Figure 5. Cyclic voltammetry curves of lithium manganate samples prepared from different values of the molar ratio of Li/Mn (n_{Li}:n_{Mn} = 1:2, 1.05:2, 1.1:2, and 1.15:2, respectively) at a scan rate of 1.0 mVs^{-1}

Table 1. Peak parameters of cyclic voltammetry curves for lithium manganate samples prepared from different values of the molar ratio of Li/Mn (n_{Li}:n_{Mn} = 1:2, 1.05:2, 1.1:2, and 1.15:2, respectively); ΔE_p is the separation between the anodic peak potential E_{pa} and the cathodic peak potential E_{pc}.

Sample	E_{pa1} (V)	E_{pa2} (V)	E_{pc1} (V)	E_{pc2} (V)	ΔE_{p1} (mV)	ΔE_{p2} (mV)
Li-1	4.183	4.352	3.774	3.926	409	426
Li-1.05	4.168	4.339	3.793	3.948	375	391
Li-1.1	4.138	4.276	3.821	4.008	317	268
Li-1.15	4.157	4.306	3.810	3.965	347	341

As shown in Table 1, compared to other three samples, Li-1.1 sample had the smallest ΔE_p meaning the fastest intercalation and deintercalation process of Li^+, and the shortened diffusion length of Li^+ [30, 31], which is the reason why Li-1.1 had the best electrochemical performance. The explanation for this phenomenon included the following aspects: (i) polyethylene glycol 12000 played a dispersant improving the dispersion of the final products; (ii) a small amount of lithium evaporation losses when temperature is high, and the amount of lithium ions inserted into the electrodes for charge neutrality determines the electrical storage capacity [23]. When the lithium resource was added too much, some impurity of $Li_{1.4}Mn_2O_4$ generated affecting the electrochemical performance of battery. Therefore, in this study, 1.1:2 was the optimal value of the molar ratio of Li/Mn.

Lithium manganate has been synthesized by many research groups and the related electrochemical data were summarized in Table 2 under different synthesizing methods. It was reported that the initial discharge capacities of lithium manganate samples prepared by solid state reaction using Mn_3O_4 and Li_2CO_3 as raw materials were108.6 (0.1 C), 105.3 (0.2 C), 100.6 (0.5 C) and

92.5 (1.0C) [13], the initial discharge capacities of lithium manganate samples synthesized via precipitation method with Li_2CO_3 and $Mn(CH_3COO)_2{\cdot}4H_2O$ as raw materials were 107 and 102 $mAhg^{-1}$ at the rate of 0.2 and 0.5 C [14]. As for the facile self-template method using $LiOH{\cdot}H_2O$, potassium permanganate, sucrose and sodium hydroxide as raw materials, the initial discharge capacities of samples reached 110.7 and 70.2 $mAhg^{-1}$ at the rates of 0.1 and 10C, respectively [19].

Table 2. Comparison of lithium manganate synthesized by different methods

Synthesizing method	Raw materials	Rate capacity ($mAhg^{-1}$)	References
High temperature ball milling	Li_2CO_3; EMD; Polyethylene glycol 12000	121.5 (0.1C); 109.5 (0.5C); 98.3 (1.0C); 86.5 (2.0C); 70.2 (5.0C)	As prepared
Solid state reaction	Mn_3O_4; Li_2CO_3	108.6 (0.1 C); 105.3 (0.2 C); 100.6 (0.5 C); 92.5 (1.0C)	[13]
Precipitation method	Li_2CO_3; $Mn(CH_3COO)_2{\cdot}4H_2O$	107 (0.2C); 102 (0.5C)	[14]
Facile self-template method	$LiOH{\cdot}H_2O$; Sucrose; Sodium hydroxide; Potassium permanganate	110.7 (0.1 C); 70.2 (10 C)	[19]

4. CONCLUSIONS

In this study, lithium manganate ($LiMn_2O_4$) was synthesized by the high temperature ball milling method with Li_2CO_3, EMD and polyethylene glycol 12000 as raw materials. Experimental results showed that some impurity of $Li_{1.4}Mn_2O_4$ could form when too much lithium resource was employed. Moreover, particles of L-1.1 (n_{Li}:n_{Mn} = 1.1:2) showed a good uniformity in shape and size. Some button batteries were assembled with the prepared lithium manganate as a cathode material, and the electrochemical performance was tested. L-1.1 exhibited the optimal electrochemical performance: initial discharge capacities were 121.5, 109.5, 98.3, 86.5 and 70.2 $mAhg^{-1}$ at rates of 0.1, 0.5, 1.0, 2.0 and 5.0 C, respectively; after 100 cycles, the capacity was 89.5 $mAhg^{-1}$ at rate of 1.0 C; the capacity retention was 91.0%.

ACKNOWLEDGMENTS
The authors gratefully acknowledge supports by the National Key R&D Program of China (No. 2017YFC0805100), the National Natural Science Foundation of China (No. 51704068), the China Postdoctoral Science Foundation (No. 2017M610184), and the Postdoctoral Foundation of Northeastern University (No. 20170305).

References

1. A. Pasquier, I. Plitz, S. Menocal and G. Amatucci, *J. Power Source*s, 115 (1) (2003) 171.
2. G. Mulder, N. Omar, S. Pauwels, M. Meeus, F. Leemans, B. Verbrugge, W.D. Nijs, P.V. Bossche, D. Six and J.V. Mierlo, *Electrochim. Acta,* 87 (2013) 473.
3. A. Eddahech, O. Briat and J. Vinassa, *Electrochim. Acta*, 114 (2013) 750.
4. E. Hosono, T. Kudo, I. Honma, H. Matsuda and H. Zhou, *Nano Lett.*, 9 (2009) 1045.
5. Z. Xiao, Y. Zhou, L. Song, F. Zhang, J. Gao, J. Zeng and Z. Cao, *J. Alloys Compd.*, 592 (2014) 226.
6. A.K. Hjelm, T. Eriksson and G. Lindbergh, *Electrochim. Acta*, 48 (2002) 171.
7. C.C Peng, J.J. Huang, Y.J. Guo, Q.L. Li, H.L. Bai, Y.H. He, C.W. Su and J.M. Guo, *Vacuum,* 120 (2015) 121.
8. D. Susanto, H. Kim, J.Y. Kim, S.H. Lim, J.W. Yang,S. A. Choi and K.Y. Chung, *Curr. Appl. Phys.*, 15 (2015) S27.
9. A.Tron, Y.D. Park and J. Mun, *J. Power Sources*, 325 (2016) 360.
10. G.H. Waller, P.D. Brooke, B.H. Rainwater, S.Y. Lai, R. Hu, Y. Ding, F.M. Alamgir, K.H. Sandhage and M.L. Liu, *J. Power Sources*, 306 (2016) 162.
11. Y.S. Shang, X.J. Lin, X. Lu, T. Huang and A.S. Yu, *Electrochim. Acta*, 156 (2015) 121.
12. T. Kozawa, K. Yanagisawa, T. Murakami and M. Naito, *J. Solid State Chem.*, 243 (2016) 241.
13. B.S. Liu, Z.B. Wang, Y. Zhang, F.D. Yu, Y. Xue, K. Ke and F.F. Li, *J. Alloys Compd.*, 622 (2015) 902.
14. G.G. Wang, J.M. Wang, W.Q. Mao, H.B. Shao, J.Q. Zhang and C.N. Cao, *J. Solid State Electrochem.*, 9 (2005) 524.
15. X.W. Lv, S.L. Chen,C. Chen, L.H. Liu, F. Liu and G.H. Qiu, *Solid State Sci.*, 31 (2014) 16.
16. G.H. Waller, S.Y. Lai, B.H. Rainwater and M.L. Liu, *J. Power Sources*, 251 (2014) 411.
17. H. Zhang, Y.L. Xu, D. Liu, X.S. Zhang and C.J. Zhao, *Electrochim. Acta*, 125 (2014) 225.
18. R.Thirunakaran, G.H. Lew and W.S. Yoon, *J. Electroanal. Chem.*, 767 (2016) 141.
19. J.Q. Den, J. Pan, Q.R. Yao, Z.M. Wang, H.Y. Zhou and G.H. Rao, *J. Power Sources*, 278 (2015) 370.
20. C.Y. Wan, M.C. Wu and D. Wu, *Powder Technol.*, 199 (2) (2010) 154.
21. D. Ke, H.G. Rong, P.Z. Dong and Q.Lu, *Electrochim. Acta*, 55 (5) (2010) 1733.
22. J.M. Tarascon and M. Armand, *Nature.*, 414 (2001) 359.
23. P.Q. Jia, Z.B. Shao and K.R. Liu, *Mater. Lett.*, 125 (2014) 218.
24. X.T. Li, Z.B. Shao, K.R. Liu, Q. Zhao, G.F. Liu and B.S. Xu, *J. Electroanal. Chem.*, 801 (2017) 368.
25. X.T. Li, Z.B. Shao, K.R. Liu, Q. Zhao, G.F. Liu and B.S. Xu, *Colloids Surf., A*, 529 (2017) 850.
26. M. Tian, X.T. Li, Z.B. Shao and F.M. Shen, *Int. J. Electrochem. Sci.*, 12 (2017) 7166.
27. Y. Xue, Z.B. Wang, F.D. Yu, Y. Zhang and G.P. Yin, *J. Mater. Chem. A,* 2 (12) (2014) 4185.
28. Y.Y. Xia and M. Yoshio, *J. Electrochem. Soc.*, 143 (1996) 825.
29. H.Q. Wang, F.Y. Lai,Y. Li, X.H. Zhang, Y.G. Huang,S.J. Hu and Q.Y. Li, *Electrochim. Acta*, 177 (2015) 290.
30. Y.C. Chen, K. Xie, Y. Pan and C.M. Zheng, *J. Power Sources*, 196 (2011) 6493.
31. H.Y. Zhao, F. Li, X.Q. Liu, W.Q. Xiong, B. Chen, H.L. Shao, D.Y. Que, Z. Zhang and Y. Wu, *Electrochim. Acta,* 166 (2015) 124.